Appl. Phys. B 82, 443–447 (2006)
DOI: 10.1007/s00340-005-2060-6

Applied Physics B
Lasers and Optics

S.W. LIU[1]
J. XU[1]
D. GUZUN[1]
G.J. SALAMO[1]
C.L. CHEN[2]
Y. LIN[2,*]
MIN XIAO[1,✉]

Nonlinear optical absorption and refraction of epitaxial $Ba_{0.6}Sr_{0.4}TiO_3$ thin films on (001) MgO substrates

[1] Department of Physics, University of Arkansas, Fayetteville, Arkansas 72701, USA
[2] The Texas Center for Superconductivity and Department of Physics, University of Houston, Texas 77204, USA

Received: 25 August 2005
Published online: 17 December 2005 • © Springer-Verlag 2005

ABSTRACT Highly epitaxial $Ba_{0.6}Sr_{0.4}TiO_3$ (BST) ferroelectric thin films were fabricated on (001) MgO substrates by pulsed laser deposition. The nonlinear optical absorption coefficients (β) and refraction indices (γ) of the BST thin films on (001) MgO substrates were investigated using the single beam Z-scan technique with femtosecond laser pulses at the wavelengths of 790 nm and 395 nm, respectively, at room temperature. The nonlinear absorption coefficients of BST thin films were measured to be ~ 0.087 cm/GW and ~ 0.77 cm/GW at 790 nm and 395 nm, respectively. The nonlinear refraction indices of BST thin films exhibit a strong dispersion from a positive value of 6.1×10^{-5} cm^2/GW at 790 nm to a negative value of -4.0×10^{-5} cm^2/GW at 395 nm near band gap. The dispersion of γ is roughly consistent with Sheik-Bahae's theory for the bound electronic nonlinear refraction resulting from the two-photon resonance. These results show that the BST film is a promising material as a candidate for nonlinear optical applications.

PACS 42.70.Mp; 78.20.-e; 81.05.-t

1 Introduction

Dielectric $Ba_{1-x}Sr_xTiO_3$ (BST) thin films have been considered to be an important material for use in tunable microwave devices such as tunable phase shifters, filters, oscillators, and antennas because of its high dielectric constant, relatively low dielectric loss tangent, and large electric field tunability [1–3]. BST thin films exhibit a large microwave tunability even up to 23.7 GHz [3], a feature that motivates the study of the nonlinear dielectric properties in optical frequency range. Recently, electro-optic (E-O) characterizations of BST films reveal an E-O coefficient with a very large saturation value of the field-induced birefringence at the wavelength of 632.8 nm [4]. Optical second-harmonic generation (SHG) has also been observed in the NIR (near infra-red) wavelength range using a high peak power Q-switched Nd-YAG laser at 1.06 μm [5] and a mode-locked Ti:Sapphire laser at 760 nm [6, 7]. Even more recently, the nonlinear optical absorption and refraction of the polycrystalline $Ba_{0.7}Sr_{0.3}TiO_3$ film on quartz substrate have been measured [8]. However, less effort has been taken to study the third-order nonlinearity of epitaxial BST thin films. The quantitative measurements of both nonlinear refraction index and adsorption coefficient of high quality epitaxial BST thin films have not been reported.

Several kinds of ferroelectric oxide thin films have already been investigated as the promising candidates for applications in nonlinear optics such as $SrBi_2Ta_2O_9$ [9], $BiMnO_3$ [10], $Bi_2Nd_2Ti_3O_{12}$ [11], PLT30 [12], (Pb, La)(Zr, Ti)O_3 [13], $PbZr_xTi_{1-x}O_3$ [14], $BaTiO_3$ [15], Ce:$BaTiO_3$ [15, 16], and Fe:$BaTiO_3$ [17]. $Ba_{0.6}Sr_{0.4}TiO_3$, a ferroelectric solid solution of $BaTiO_3$ and $SrTiO_3$, is nominally in its paraelectic state at room temperature. $Ba_{0.6}Sr_{0.4}TiO_3$ thin films are highly transparent from near ultraviolet to infrared. The Curie temperature of (Ba, Sr)TiO_3 may be continuously tailored by selecting different mole content ratio of Ba and Sr. This versatile property enhances the potential applications of (Ba, Sr)TiO_3 in different temperature environments. Compared to lead-contained ferroelectrics where lead is a volatile constituent and poisonous, (Ba, Sr)TiO_3 is non-volatile and easy to be fabricated. Moreover, (Ba, Sr)TiO_3 thin films are compatible with various microwave devices, which are beneficial to the future integration of optoelectronics with microwave electronics.

2 Experimental details

Dielectric $Ba_{0.6}Sr_{0.4}TiO_3$ thin films were grown by using pulsed laser ablation by a KrF excimer laser with a wavelength of 248 nm. An energy density of ~ 2.5 J/cm^2 and a repetition rate of $5 \sim 10$ Hz were used for the film deposition. A stoichiometric BST (60:40) target with a density of 95% was used. Since the Z-scan technique is sensitive to crystalline defects, surface imperfections, and inhomogeneities, single-crystal double-side polished (001) cubic MgO substrates were selected for the epitaxial growth of BST thin films. Such substrates maintain excellent crystalline quality and are still highly transparent even when they are heated for more than one hour at the deposition temperature (higher than 820 °C) in a low oxygen-pressure chamber environment ($200 \sim 300$ mTorr). The crystalline quality and epitaxial behavior of the as-grown BST thin films were characterized

✉ Fax: 479-5754580, E-mail: mxiao@uark.edu
*_Moved to:_ Superconductivity Technology Center, Los Alamos National Laboratory, Los Alamos, New Mexico 87545, USA

using both X-ray diffraction and transmission electron microscopy techniques. The linear optical parameters of BST thin films such as the refraction index, linear absorption coefficient and band-gap energy were extracted from the transmittance spectrum using the envelope technique [18]. The nonlinear optical measurements were performed using a single beam Z-scan technique [19]. The nonlinear optical absorption and refraction at both the wavelengths of 790 nm and 395 nm were measured to indicate their dispersion with the wavelength. The light source was a mode-locked Ti:Sapphire laser with a low repetition rate of 250 KHz at the wavelength of 790 nm, which has a temporal width of about 60 femtosecond and a peak power up to 13 MW. The 395 nm pulse laser beam was achieved by frequency doubling with a peak power up to 1.6 MW. Both output beams were collimated and expanded. Their spatial profiles at both 790 nm and 395 nm were determined to be approximately Gaussian. The beams were then focused by a lens with a focal length of 80 mm to achieve the focal waist radii of $\omega_0 \sim 11\,\mu$m ($z_0 = 0.5$ mm) at 790 nm and 7 μm ($z_0 = 0.4$ mm) at 395 nm, respectively, as determined from the measured beam divergences. To reduce the effect of noise due to the fluctuations in the pulse energy, another detector was used to monitor the pulse energy as a reference. All closed-aperture (CA) Z-scan measurements were performed with a fixed linear transmittance of $S = 20\%$, defined as the fraction of the beam energy passing through the far-field aperture. The open-aperture (OA) and closed-aperture (CA) Z-scan traces may be fitted by two corresponding numerical programs based on [19] to obtain the nonlinear optical absorption coefficient β and the nonlinear refraction index γ. The sample's parameters of α (linear optical absorption coefficient) and L (sample thickness), as well as the laser's parameters of R (repetition rate), t_{FWHM} (FWHM of pulse's duration), and AP (average incidence power of the laser beam) are required as the inputs for these numerical programs. The peak power (PP) of the laser pulse is calculated via the formula $PP = \frac{2\sqrt{\ln 2}}{\sqrt{\pi}} \frac{AP}{R \cdot t_{\mathrm{FWHM}}}$.

3 Results and discussions

3.1 *Structure properties*

The X-ray diffraction pattern (Fig. 1) of the $\theta - 2\theta$ scan along the surface of BST thin film shows that only BST (00l)-type reflections together with the corresponding reflections from MgO (001) substrate appear, indicating that the as-grown film is c-axis aligned. The rocking θ scan from (002) reflection of the BST film, as shown in the inset of Fig. 1, reveals that the tilt distribution of the film crystallites is very narrow with a FWHM of about 0.5°. Further microstructure studies from the cross-sectional TEM show the BST films exhibit columnar-like growth with the surface roughness on the order of 5 nm. Details of the deposition conditions and structural characterizations for the BST thin films were described in [3].

3.2 *Linear optical properties*

The optical transmittance spectrum of the BST film on a MgO substrate in the wavelength range of 200–1000 nm is shown in Fig. 2. The film is highly transparent in the visible

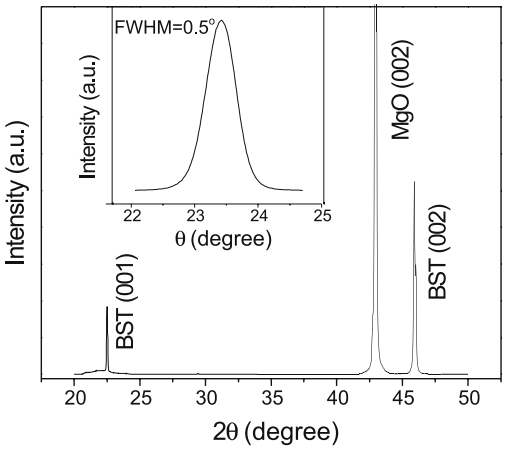

FIGURE 1 X-ray diffraction pattern of $\theta \sim 2\theta$ scan along the surface normal to the BST film on (001) MgO substrate. The inset is a rocking curve measurement from the (002) BST reflection

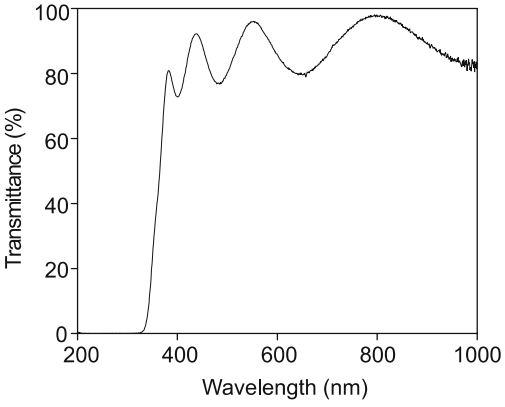

FIGURE 2 Optical transmittance spectrum of BST thin film on a MgO substrate

region with the transmittance up to 98%. The transparency of the BST film drops sharply in the UV region and the absorption edge is located at about 328 nm. The film's thickness and the linear refraction index n_0 were obtained from the transmittance spectrum using the envelope technique [18]. The film's thickness was calculated to be about 420 nm. The linear refraction indices n_0 at both wavelengths of 790 nm and 395 nm were determined to be 2.20 and 2.27, respectively. The linear absorption constant α at 395 nm was estimated to be 3237 cm^{-1} from the transmittance spectrum using the relation

$$\alpha = \frac{\ln(1/T_\alpha)}{d}, \tag{1}$$

where T_α is the interference-free transmittance [18] of the thin film after subtracting the substrate's absorption. The substrate's absorption constant was estimated to be 0.2 cm^{-1} at 790 nm and 11.0 cm^{-1} at 395 nm via the optical transmittance measurement on a 0.5 mm thick MgO substrate. The optical band gap energy E_{g} of BST, calculated by applying Tauc relation [20] $(\alpha h\upsilon)^2 = \mathrm{cons\,tan}\,t \times (h\upsilon - E_{\mathrm{g}})$, is about 3.64 eV. The small linear absorption coefficient of BST film at 790 nm is out of the sensitivity range of our transmittance measurements. We adopted the same value 0.2 cm^{-1} as the MgO substrate's linear absorption coefficient to fit the Z-scan

traces. It was found that the Z-scan traces for BST film were insensitive to the small α in a large range of values, and, therefore, this assumption has no significant error for extracting the nonlinear optical constants.

3.3 *Nonlinear optical absorption and refraction measurements*

OA and CA Z-scan measurements were first performed on a 0.5 mm MgO substrate. Figure 3a shows the typical OA Z-scan trace with an average incidence power of $AP = 198$ mW ($PP = 12.40$ MW) at the wavelength of 790 nm. The optical loss due to Fresnel reflection on the MgO surface has been taken into account. The trace exhibits a symmetric valley with respect to the focus, indicating that the MgO substrate possesses the positive nonlinear optical absorption. Fig. 3b shows a typical CA Z-scan trace with the same laser power at 790 nm. The typical valley preceding the peak indicates a positive nonlinear optical refraction (self-focusing). The nonlinear absorption coefficient β and the nonlinear refraction index γ were determined to be 3.3×10^{-4} cm/GW and 5.7×10^{-8} cm^2/GW, respectively, using the numerical fitting. The OA and CA Z-scan measurements at the wavelength of 395 nm with $AP = 18.2$ mW ($PP = 1.14$ MW) are also shown in Fig. 3c and d, respectively. The nonlinear optical parameters (β, γ) at 395 nm were determined to be (2.0×10^{-3} cm/GW, 2.4×10^{-7} cm^2/GW) by numerical fitting. Since the MgO crystal has an extremely large band-gap energy (7.7 eV) $E_g > 2\hbar\omega$, the two-photon absorption should vanish for both wavelengths of 790 nm and 395 nm. We believe that the non-zero nonlinear optical absorption coefficients are associated with the impurity levels between the valance band and conduction band [13] or are due to the higher order processes because under our experimental conditions the peak irradiance reaches as high as several thousand gigawatts per centimeter square.

Figure 4 shows the Z-scan measurements for the BST thin film on a 0.3 mm MgO substrate at the wavelength of 790 nm. The total average incidence power (AP) of the laser beam is 212.7 mW. If the Fresnel reflection on the BST film is taken into account, the incidence power entering the BST film is reduced to 182.7 mW. The incidence power on the interface between the BST film and the MgO substrate is 179.8 mW after further subtracting the losses due to Fresnel reflection at the interface and the small linear absorption in the BST thin film. The solid squares in Fig. 4a represent the measured OA data for the BST/MgO sample. Without considering the nonlinear absorption of the BST film the solid squares are fitted with the solid line via the parameters $\alpha = 0.2$ cm^{-1}, $L = 0.3$ mm, $AP = 179.8$ mW, and $\beta = 4.6 \times 10^{-4}$ cm/GW, which is larger than that of the pure MgO substrate. The dotted line is the numerical OA Z-scan trace for a 0.3 mm MgO substrate with the same input power of $AP = 179.8$ mW. The enhanced valley from BST/MgO compared to the OA trace from only MgO substrate is due to the nonlinear absorption of the BST film. The pure OA Z-scan signal (open squares in Fig. 4b) from only the BST film was extracted by subtracting the MgO substrate's signal (dotted line in Fig. 4a) from the total Z-scan signal (solid line in Fig. 4a). The nonlinear absorption coefficient of the BST film was then determined to be 0.087 cm/GW by fitting the open squares using the film's parameters $\alpha = 0.2$ cm^{-1}, $L = 420$ nm, and $AP = 182.7$ mW. This small nonlinear absorption coefficient is believed to have a similar mechanism as for MgO because the direct two-photon absorption between valance band and conduction band is forbidden ($E_g/\hbar\omega = 2.3$). The same method could be used to deduce the nonlinear optical refraction index of the BST film from the CA Z-scan measurement. As shown in Fig. 4c, the measured CA Z-scan trace (full squares)

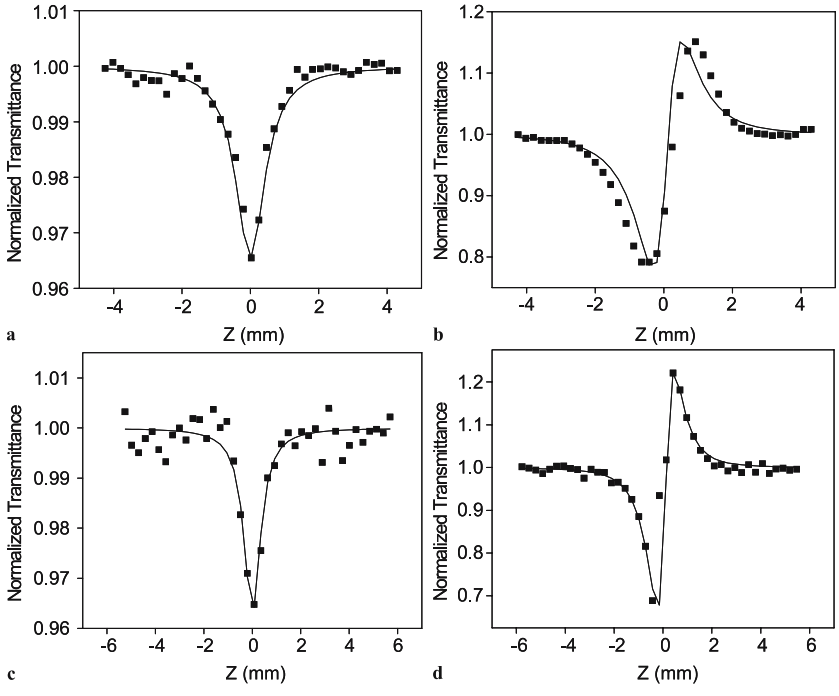

FIGURE 3 Measured Z-scan traces of a 0.5 mm (001) MgO substrate using 60 fs laser pulses with focus waist radii 11 μm at 790 nm and 7 μm at 395 nm. The *solid squares* are the measured data and the *solid lines* are the theoretical fits for (**a**) OA trace at 790 nm; (**b**) CA trace at 790 nm; (**c**) OA trace at 395 nm; (**d**) CA trace at 395 nm

from the BST/MgO sample may be numerically fitted via the parameters $\alpha = 0.2\,\mathrm{cm}^{-1}$, $L = 0.3$ mm, $AP = 179.8$ mW, $\beta = 4.0 \times 10^{-4}$ cm/GW and $\gamma = 1.4 \times 10^{-7}\,\mathrm{cm}^2/\mathrm{GW}$ without considering the nonlinear refraction of the BST film. It exhibits a much higher valley-to-peak value than that of the MgO substrate's signal (dotted line). The effect may be attributed to the positive nonlinear refraction of the BST film. The extracted CA Z-scan data (open squares in Fig. 4d) for the BST film, which were obtained by subtracting the dotted line from the solid line in Fig. 4c, were numerically fitted with the film's parameters $\beta = 0.087$ cm/GW, $L = 420$ nm, $AP = 182.7$ mW, and $\gamma = 6.1 \times 10^{-5}\,\mathrm{cm}^2/\mathrm{GW}$.

The Z-scan measurements at the wavelength 395 nm were also performed on BST/MgO film with $AP = 21.2$ mW after subtracting the loss due to the Fresnel reflection on the BST surface. The AP on the interface between the BST film and the MgO substrate is reduced to 18.2 mW after further subtracting the strong linear absorption in BST film and Fresnel reflection in the interface. As shown in Fig. 5a, the OA Z-scan trace from the BST/MgO sample exhibits a strongly enhanced valley indicating a positive nonlinear absorption for BST film. The pure OA Z-scan data (open squares) from BST film were extracted from these measurements shown in Fig. 5b. The nonlinear absorption coefficient was determined

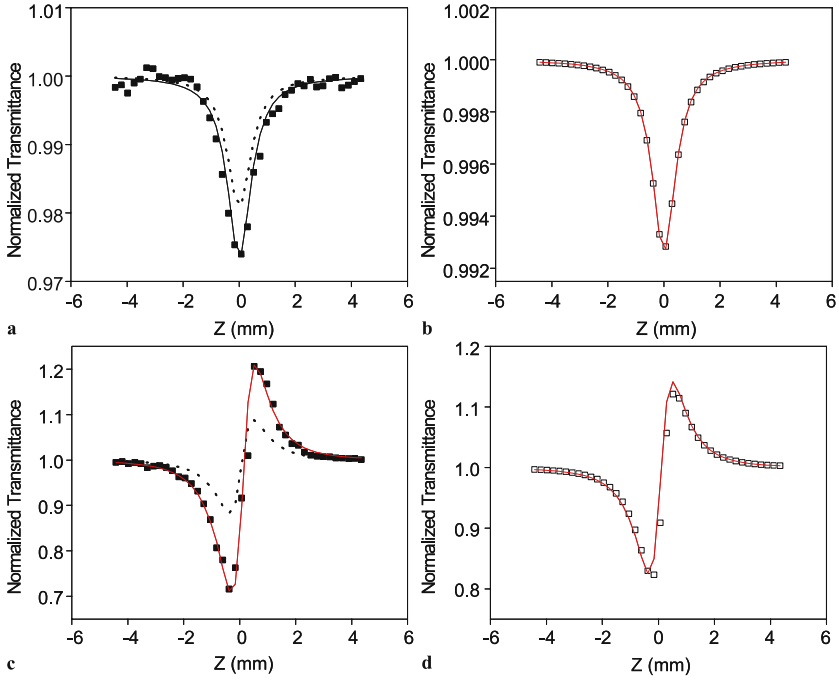

FIGURE 4 Z-scan measurements of BST film on a 0.3 mm (001) MgO substrate at the wavelength of 790 nm. The *solid squares* are the measured data from BST/MgO. The *open squares* are the deduced data of BST film. The *solid lines* are the numerical fits for *solid squares*. The *dotted lines* are the numerical traces from only MgO substrate. (**a**), (**b**) OA traces and (**c**), (**d**) CA traces

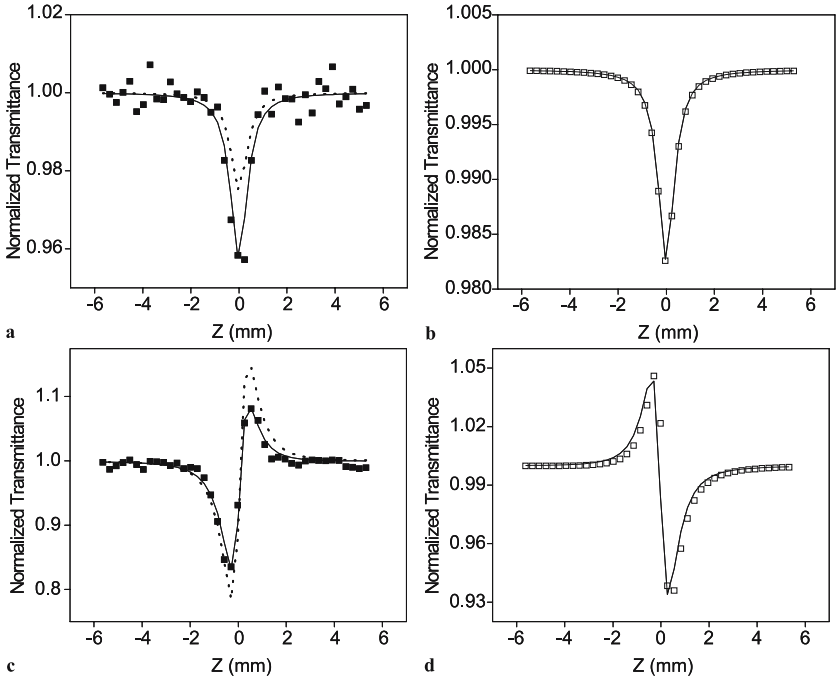

FIGURE 5 Z-scan measurements of BST film on a 0.3 mm (001) MgO substrate at the wavelength of 395 nm. The *solid squares* are the measured data from BST/MgO. The *open squares* are the deduced data of BST film. The *solid lines* are the numerical fits for *solid squares*. The *dotted lines* are the numerical traces from only MgO substrate. (**a**), (**b**) OA traces and (**c**), (**d**) CA traces

to be 0.77 cm/GW for the BST film. As shown in Fig. 5c, the CA signal exhibits a lower peak-to-valley value, which indicates that the BST film has a negative nonlinear refraction index at 395 nm. The CA Z-scan data (open squares) as shown in Fig. 5d from BST thin film were obtained by subtracting the dotted line from the solid line in Fig. 5c. The nonlinear refraction index was determined to be $-4.0\times10^{-5}\,\mathrm{cm}^2/\mathrm{GW}$ by numerical fitting. The negative refraction index in the near band edge is consistent with the Sheik-Bahae's dispersion theory [21, 22] for the bound electronic nonlinear refraction resulting from a two-photon resonance in solids. The bound electronic nonlinearity in solids depends only on the ratio of the photon energy ($\hbar\omega$) to the band gap energy (E_g) of the material as described by [21]

$$\gamma = K\frac{\hbar c\sqrt{E_\mathrm{p}}}{2n_0^2E_\mathrm{g}^4}G_2[\frac{\hbar\omega}{E_\mathrm{g}}]\,, \tag{2}$$

where the dispersion function $G_2(x)$ is given by

$$G_2(x) = \frac{1}{(2x)^6}[-2+6x-3x^2-x^3-0.75x^4-0.75x^5 + 2(1-2x)^{3/2}\Theta(1-2x)]\,, \tag{3}$$

with $\Theta(x)$ being Heaviside step function. The ratio of γ at the wavelength of 395 nm to γ at the wavelength of 790 nm is calculated via (2) to be -0.52, which has a 21% error compared to the experimentally measured value of -0.66.

4 Conclusion

We investigated the optical nonlinearity of the epitaxial $Ba_{0.6}Sr_{0.4}TiO_3$ (BST) thin film and (001) MgO substrate by the single beam Z-scan technique using femtosecond laser pulses at the wavelengths of 790 nm and 395 nm, respectively. The nonlinear optical absorption coefficients and the nonlinear refraction indices of BST films were extracted by subtracting the MgO substrate's effects from the total Z-scan signal of BST/MgO. The third-order nonlinear optical parameters (β, γ) were determined to be ($0.087\,\mathrm{cm/GW}$, $6.1\times10^{-5}\,\mathrm{cm}^2/\mathrm{GW}$) at 790 nm and ($0.77\,\mathrm{cm/GW}$, $-4.0\times10^{-5}\,\mathrm{cm}^2/\mathrm{GW}$) at 395 nm, respectively. The dispersion behavior of the nonlinear refraction indices at these two wavelengths are roughly consistent with the bound electronic nonlinear refraction predicted by two-photon resonance. These results indicate that the ferroelectric BST film is a promising material as a candidate for nonlinear optical applications.

ACKNOWLEDGEMENTS The work was partially funded by a grant from Army Research Laboratory.

REFERENCES

1 C.L. Chen, H.H. Feng, Z. Zhang, A. Brazdeikis, F.A. Miranda, F.W. Van Kewls, R.R. Romanofsky, Z.J. Huang, Y. Liou, W.K. Chu, C.W. Chu, Appl. Phys. Lett. **75**, 412 (1999)
2 B.H. Park, Y. Gim, Y. Fan, Q.X. Jia, P. Lu, Appl. Phys. Lett. **77**, 2587 (2000)
3 C.L. Chen, J. Shen, S.Y. Chen, G.P. Luo, C.W. Chu, F.A. Miranda, F.W. Van Keuls, J.C. Jiang, E.I. Meletis, H.Y. Chang, Appl. Phys. Lett. **78**, 652 (2001)
4 D.-Y. Kim, S.E. Moon, E.-K. Kim, S.-J. Lee, J.-J. Choi, H.-E. Kim, Appl. Phys. Lett. **82**, 1455 (2003)
5 J.F. Scott, A.Q. Jiang, S.A.T. Redfem, M. Zhang, M. Dawber, J. Appl. Phys. **94**, 3333 (2003)
6 E.D. Mishina, N.E. Sherstyuk, D.R. Barskiy, A.S. Sigov, Yu.I. Golovko, V.M. Mukhorotov, M. De Santo, Th. Rasing, J. Appl. Phys. **93**, 6216 (2003)
7 E.D. Mishina, N.E. Sherstyuk, V.I. Stadnichuk, A.S. Sigov, V.M. Mukhorotov, Yu.I. Golovko, A. van Etteger, Th. Rasing, Appl. Phys. Lett. **83**, 2402 (2003)
8 Peng Shi, Xi Yao, Liangying Zhang, Xiaoqing Wu, Mingqiang Wang, Xin Wan, Sol. Stat. Comm. **134**, 589 (2005)
9 W.F. Zhang, M.S. Zhang, Z. Yin, Y.Z. Gu, Z.L. Du, B.L. Yu, Appl. Phys. Lett. **75**, 902 (1999)
10 A. Sharan, I. An, C. Chen, R.W. Collins, J. Lettieri, Y. Ji, Appl. Phys. Lett. **83**, 5169 (2003)
11 B. Gu, Y.-H. Wang, X.-C. Peng, J.-P. Ding, J.-L. He, H.-T. Wang, Appl. Phys. Lett. **85**, 3687 (2004)
12 Q. Zhao, Y. Liu, W. Shi, W. Ren, L. Zhang, X. Yao, Appl. Phys. Lett. **69**, 458 (1996)
13 W.F. Zhang, Y.B. Huang, M.S. Zhang, Appl. Surf. Sci. **158**, 185 (2000)
14 P. Yang, J. Xu, J. Ballato, R.W. Schwartz, D.L. Carroll, Appl. Phys. Lett. **80**, 3394 (2002)
15 W.F. Zhang, Y.B. Huang, M.S. Zhang, Z.G. Liu, Appl. Phys. Lett. **76**, 1003 (2000)
16 L.-z. Xuan, S.-h. Pan, Z.-h. Chen, R.-p. Wang, W.-s. Shi, C.-l. Li, Appl. Phys. Lett. **73**, 2896 (1998)
17 W. Wang, G. Yang, Z. Chen, Y. Zhou, H. Lu, G. Yang, J. Opt. Soc. Am. B **20**, 1342 (2003)
18 R. Swanepoel, J. Phys. E: Sci. Instrum. **16**, 1214 (1983)
19 M. Sheik-bahae, A.A. Said, T.-h. Wei, D.J. Hagan, E.W. Van Stryland, IEEE J. Quantum Electron. **QE-26**, 760 (1990)
20 D.Y. Wang, C.L. Mak, K.H. Wong, H.L.W. Chan, C.L. Choy, Ceram. Intern. **30**, 1745 (2004)
21 M. Sheik-Bahae, D.J. Hagan, E.W. Van Stryland, Phys. Rev. Lett. **65**, 96 (1990)
22 M. Sheik-Bahae, D.C. Hutchings, E.W. Van Stryland, IEEE J. Quantum Electron. **QE-27**, 1296 (1991)